

# Generation of lattice structures of optical vortices

Alexander Dreischuh and Sotir Chervenkov

*Department of Quantum Electronics, Sofia University, 5 James Bourchier Blvd, 1164 Sofia, Bulgaria*

Dragomir Neshev

*Laser Centre, Vrije Universiteit Amsterdam, De Boelelaan 1081, 1081 HV Amsterdam, The Netherlands*

Gerhard G. Paulus

*Max-Planck-Institut für Quantenoptik, Hans-Kopfermann-Strasse 1, D-85748 Garching, Germany*

Herbert Walther

*Max-Planck-Institut für Quantenoptik, Hans-Kopfermann-Strasse 1, D-85748 Garching, Germany, and Sektion Physik, Ludwig-Maximilians-Universität München, Am Coulombwall 1, D-85748 Garching, Germany*

Received April 27, 2001; revised manuscript received September 4, 2001

We demonstrate experimentally the generation of square and hexagonal lattices of optical vortices and reveal their propagation in a saturable nonlinear medium. If the topological charges of the vortices have identical signs, the lattice exhibits rotation, whereas if their signs alternate between being the same and being opposite to each other, we observe stable propagation of the structures. In the nonlinear medium the lattices induce periodic modulation of the refractive index. Diffraction of a probe beam by this nonlinearity-induced periodic structure is observed. © 2002 Optical Society of America

*OCIS codes:* 190.4420, 230.4320.

## 1. INTRODUCTION

Optical vortices are intriguing objects that attract much attention<sup>1</sup> and display fascinating properties with possible applications in the optical transmission of information and in guiding and trapping of particles. They have a characteristic screw-type phase dislocation<sup>2</sup> whose order multiplied by its sign is referred to as a topological charge (TC). The study of optical vortices and, in general, phase singularities not only suggests new directions for fundamental research but also provides links to other branches of physics, such as quantum optics,<sup>3</sup> superfluidity,<sup>4</sup> Bose–Einstein condensates,<sup>5,6</sup> and cosmology.

Optical vortices can be generated in several different controllable ways: in lasers with large Fresnel numbers<sup>7</sup> or by helical phase plates,<sup>8</sup> laser mode converters,<sup>9,10</sup> and computer-generated holograms (CGHs).<sup>11</sup> The method of CGHs, however, is the most commonly used, because it permits precise control of the vortex position and the TC and provides a possibility of generation of desired patterns of optical vortices.

The propagation dynamics of a single vortex, in both linear and nonlinear media, has been the subject of much research (see, e.g., Refs. 12–14), in which also the noncanonical properties of the vortex have been taken into account.<sup>15,16</sup> It has been shown that the vortex position on a background beam is strongly affected by any source of phase and intensity gradients<sup>17–19</sup> and can be controlled by interference with a weak plane wave.<sup>20</sup> If the

vortices propagate in self-defocusing nonlinear media (NLMs), they can form an optical vortex solitons (OVSs).<sup>21</sup> (For an overview of OVSs see Ref. 1, Chaps. 7 and 8.) In a NLM, OVSs induce optical waveguides in a medium<sup>22–24</sup> that can guide weak information beams. An OVS was experimentally generated first in a Kerr NLM<sup>25</sup> and later in media with other types of nonlinearity: saturable-atomic,<sup>26</sup> photorefractive,<sup>27</sup> and photovoltaic.<sup>28</sup> Recently an OVS was observed in a quadratic NLM with a defocusing response. However, care was taken to avoid modulational instability of the plane-wave background beam.<sup>29</sup>

The propagation of multiply charged OVSs has also been investigated.<sup>30,31</sup> It was found that they are topologically unstable and decay into vortices of unit charge.<sup>32</sup> The vortices produced by the decay can arrange themselves into regular patterns (vortex ensembles) while they interact with one another by means of phase and intensity gradients. The decay of the higher-order vortices obeys the general principle of conservation of the total angular momentum (AM) of the beam that carries them. Additionally, for a closed region of space the net topological charge must be conserved during continuous evolution, provided that no vortices enter or leave the region.

An ensemble of optical vortices exhibits a fluidlike motion<sup>18,33</sup> that depends strongly on the geometrical configuration. The propagation of the simplest vortex ensemble, namely, a vortex pair, has been investigated by several groups of researchers.<sup>17,18,33–35</sup> In Ref. 34 the ro-

tation of a pair of vortices with equal TCs is reported to be controlled by the Gyou phase of the host Gaussian beam. Changing the beam intensity changes the position of the beam waist inside the self-defocusing NLM, thus changing the angle of rotation at the output plane. A comparison between the degree of rotation of a vortex pair in linear and nonlinear regimes was made in Ref. 35. It was pointed out that the effect of rotation in the nonlinear regime can be more than three times greater than in the linear regime. The enhancement is assigned to the nonlinear confinement of the vortex cores, which allows the vortices to propagate as vortex filaments.

Recently the propagation of vortex arrays was investigated. Such arrays were generated by a bent glass plate<sup>36</sup> or as a result of transverse instability of dark-soliton stripes.<sup>37–39</sup> The instability could be enhanced additionally when the dark-soliton stripe interacted with an optical vortex, causing unzipping of the stripe.<sup>40</sup> Ensembles of ordered optical vortices were also investigated in quadratic NLMs and promise controllable generation of multiple-vortex patterns.<sup>41</sup> The proposed method paves the way for creation of reconfigurable vortex ensembles by means of seeded second-harmonic generation.

With respect to the fluidlike motion of the vortex ensembles, a stationary configuration of vortices was found.<sup>33</sup> It consists of three vortices of equal TC situated in an equilateral triangle and an additional vortex with an opposite TC in the center. That configuration proved to be stable to small displacement of one of the dislocations. However, if the vortices are of higher order they decay and subsequently form another stationary configuration, which resembles part of a hexagonal honeycomb lattice. This fact directs our attention to the investigation of optical vortex lattices and to characterization of the propagation of the beams upon which they are imposed.

Until now, lattices of optical vortices propagating in NLMs were considered only theoretically. The simplest case of a square lattice consisting of vortices with alternating charges was investigated by direct modeling of four vortices under periodic boundary conditions.<sup>42</sup> Later, lattices with different geometries superimposed upon a finite background beam (conditions closer to experimental ones) were considered.<sup>33</sup> It was shown that, depending on the TCs, the vortex lattices can exhibit rotation or rigid propagation for equal or alternating TCs, respectively. In addition, lattices possess elasticity against displacement of one or more vortices out of their equilibrium positions.

Here we report what is to our knowledge the first experimental investigation of lattice structures of optical vortices in self-defocusing NLMs. We concentrate our attention on two types of lattice geometry, square and hexagonal. When beams propagate in a NLM they induce a periodic modulation of the medium's refractive index. For high beam intensities these changes are sufficient to cause diffraction of a probe beam propagating perpendicularly to the volume with a periodically modulated refractive index. One may control this diffraction by steering the propagation of the vortex lattice, e.g., by controlling its degree of rotation (for lattices that consist of vortices with equal charges). One may attain additional control

by changing the pump beam's intensity, which changes the refractive index of the medium and therefore the diffraction efficiency of the induced periodic phase grating.

The maximal refractive-index change in our experiment is of the order of  $10^{-4}$  to  $10^{-3}$ , which is not enough to permit an effective two-dimensional photonic bandgap structure to be formed.<sup>43</sup> As a proof of principle, however, one can consider the possibility of trapping glass spheres<sup>44</sup> by using optical vortices ordered in a lattice. This might give an opportunity for generation of effective two-dimensional photonic crystals. One could reconfigure such a crystal by altering the degree of rotation of the lattice (by changing the intensity of the focused background beam as described in Ref. 34) for equal TCs or by use of dynamically reconfigurable holograms.<sup>45</sup>

We would like to emphasize the close link between our results and those found in the field of Bose–Einstein condensates, for which experimental investigations of vortex ensembles,<sup>46</sup> vortex arrays as a result of dark soliton-stripe instability,<sup>47</sup> and vortex lattices<sup>48</sup> have been reported recently.

## 2. GENERAL ANALYSIS

Let us consider the propagation of a beam in a self-defocusing NLM with saturable nonlinearity whose evolution is described by the normalized nonlinear Schrödinger equation for the slowly varying amplitude envelope:

$$i \frac{\partial E}{\partial z} + \frac{1}{2} \Delta_{\perp} E - \frac{|E|^2 E}{(1 + s|E|^2)^{\gamma}} = 0, \quad (1)$$

where  $\Delta_{\perp}$  is the transverse Laplace operator. The transverse coordinates  $(x, y)$  are normalized to the characteristic size of the dark structures  $a$ , and the propagation coordinate  $z$  is normalized to the diffraction length of the dark beams. The background beam intensity  $I = |E|^2$  is expressed in units of the intensity necessary for forming a one-dimensional dark soliton  $I_{1\text{Dsol}}$  of size  $a$ . The saturation parameter is defined by  $s = I_{1\text{Dsol}}/I_{\text{sat}}$ , where  $I_{\text{sat}}$  is the saturation intensity retrieved by the experimental conditions. We introduce phenomenologically the model of the saturation that we use to describe the nonlinear response of the thermal medium. The model was derived from a test experiment for self-bending of the background beam and was described in detail in Refs. 32 and 49. The parameters of nonlinear response functions  $s$  and  $\gamma$  depend on the particular conditions in which the experiment is performed, e.g., on the properties of the NLM and on the focusing conditions. In all measurements reported here we used thermal nonlinearity and, in particular, ethylene glycol dyed with DODCI (diethyloxadicarbocyanine iodide). Two concentrations of the dye were used, so  $s = 0.4, 1.2$ ;  $\gamma \approx 3$  in both cases.

To investigate the propagation dynamics of vortex lattices we first conducted numerical simulations by using the beam propagation method. The initial conditions were modeled as the superposition of vortices situated in the nodes of a lattice:

$$E(\mathbf{r}, z = 0) = \prod_{j,k=-\infty}^{\infty} \begin{cases} \text{sq}(\mathbf{r} - \mathbf{r}_{jk}) \\ \text{hex}(\mathbf{r} - \mathbf{r}_{jk}) \end{cases}, \quad (2)$$

with square (sq) and hexagonal (hex) symmetry. In Eq. (2),  $\mathbf{r}_{jk}$  are the nodes of the Bravais lattice that represents the physical lattice structure. The square lattice (Fig. 1, top row) coincides with the Bravais lattice; however, the hexagonal honeycomb lattice (Fig. 1, middle row) is represented by a Bravais lattice with a base containing two vortices. If one defines the primitive vectors of the Bravais lattice as  $\mathbf{b}$  and  $\mathbf{c}$ , then the nodes of the lattice are described as  $\mathbf{r}_{jk} = j\mathbf{b} + k\mathbf{c}$ , where  $j$  and  $k$  are integers. The primitive vectors of the square lattice are orthogonal to each other and can be expressed in  $(x, y)$  coordinates as  $\mathbf{b} = (\Delta, 0)$  and  $\mathbf{c} = (0, \Delta)$ , where  $\Delta$  is the distance between two neighboring vortices. For the honeycomb lattice the primitive vectors are not orthogonal and are expressed as  $\mathbf{b} = (\sqrt{3}\Delta, 0)$  and  $\mathbf{c} = [(\sqrt{3}/2)\Delta, (3/2)\Delta]$ . Then the two vortices inside the elementary cell have positions  $\mathbf{r}_1 = 1/3(\mathbf{b} + \mathbf{c})$  and  $\mathbf{r}_2 = 2/3(\mathbf{b} + \mathbf{c})$ .

The functions  $\text{sq}(\mathbf{r} - \mathbf{r}_{jk})$  and  $\text{hex}(\mathbf{r} - \mathbf{r}_{jk})$  describe the structure of the elementary cell of the Bravais lattice and are expressed as

$$\text{sq}(\mathbf{r} - \mathbf{r}_{jk}) = \tanh(|\mathbf{r} - \mathbf{r}_{jk}|) \times \exp\left[i \text{sgn}^{j+k} \arctan \frac{(\mathbf{r} - \mathbf{r}_{jk})_y}{(\mathbf{r} - \mathbf{r}_{jk})_x}\right], \quad (3)$$

$$\begin{aligned} \text{hex}(\mathbf{r} - \mathbf{r}_{jk}) &= \tanh(|\mathbf{r} - \mathbf{r}_{jk} - \mathbf{r}_1|) \tanh(|\mathbf{r} - \mathbf{r}_{jk} - \mathbf{r}_2|) \\ &\times \exp\left[i \arctan \frac{(\mathbf{r} - \mathbf{r}_{jk} - \mathbf{r}_1)_y}{(\mathbf{r} - \mathbf{r}_{jk} - \mathbf{r}_1)_x}\right] \\ &\times \exp\left[i \text{sgn} \arctan \frac{(\mathbf{r} - \mathbf{r}_{jk} - \mathbf{r}_2)_y}{(\mathbf{r} - \mathbf{r}_{jk} - \mathbf{r}_2)_x}\right]. \end{aligned} \quad (4)$$

The sign function (sgn) is equal to +1 for equal TCs and to -1 for alternating TCs.

Then the lattice structure is superimposed upon a super-Gaussian (flat-topped) background beam:

$$B(x, y, z = 0) = \sqrt{I_0} \exp\left[-\left(\frac{\sqrt{x^2 + y^2}}{w}\right)^{14}\right], \quad (5)$$

where width  $w$  is chosen to exceed the characteristic width of the dark structures  $a$  more than 40 times and  $I_0$  is the maximal background beam intensity.

We modeled the propagation of lattices of different geometries and different TC distributions (see Fig. 1). No qualitative differences were observed in the propagation of vortex structures with respect to the lattice geometry (square or hexagonal). The propagation, however, depends crucially on the vortex charge distribution [equal, Fig. 1(b), or alternating, Fig. 1(c)]. Two characteristic differences can be clearly seen: (i) In the case of equal TCs (sgn = +1) the superposition of the phases of all vortices results in an azimuthal phase gradient and a non-zero total AM, which causes rotation of the whole structure [Fig. 1(b)]. In the case of alternating TCs (sgn = -1) the superposition of all the phases gives, on average, no phase gradient and zero total AM. As a result, steady propagation of the lattice is observed in the simulations [Fig. 1(c)]. (ii) In the case of equal TCs the non-zero total AM and the centrifugal forces lead to increased broadening of the background beam. The maximal in-

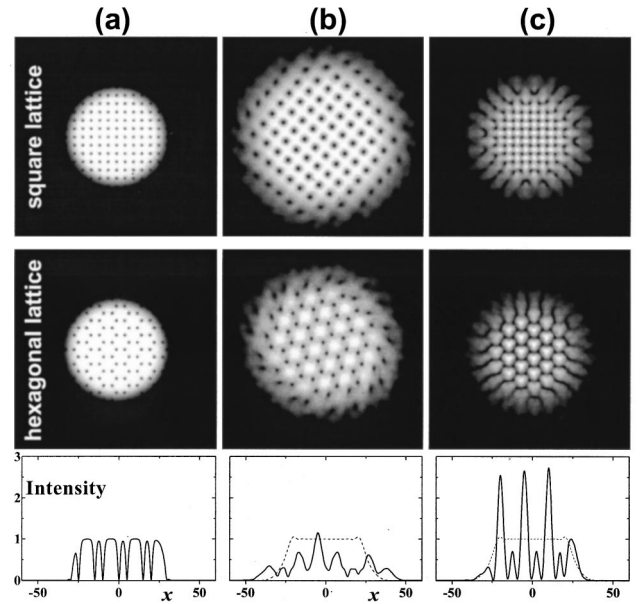


Fig. 1. Background beams containing vortex lattices of different geometries: (a) at the input of the NLM and (b), (c) at  $z = 10$  for lattices with equal and alternating TCs, respectively. Images of square-shaped and hexagonal lattices are shown. Bottom, transverse slices of hexagonal lattices. For comparison, a transverse slice of the background beam (without vortices imposed) is shown by dashed curves. In all cases  $\Delta = 5.0$ ,  $I_0 = 1$ , and  $s = 0.4$ . The images are gray-scale coded; white corresponds to maximal intensity.

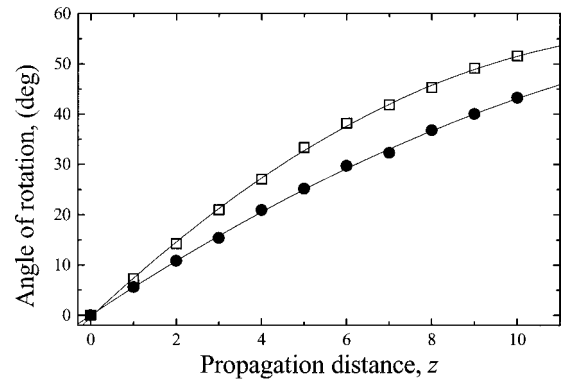


Fig. 2. Angles of rotation of vortex lattices of equal TCs versus propagation distance for square (open squares) and hexagonal (filled circles) geometry. Solid curves are guides for the eye. The lattice parameters are the same as in Fig. 1.

tensity rapidly decreases along the NLM [ $I \approx 0.6$  at  $z = 10$  Fig. 1(b), bottom]. The dependence of the beam propagation on the intensity in this case is relatively weak, and topological effects dominate nonlinear effects. In the case of alternating TCs [Fig. 1(c)] the background beam broadening is an effect that is due only to the combined action of diffraction and self-defocusing nonlinearity and depends strongly on the beam's intensity.

The degrees of rotation of the two lattice geometries for equal TCs are depicted in Fig. 2. The rotation is due to the phase gradient, which is greater for the denser (square-shaped) structure. Therefore the rotation of the square structure (open squares in Fig. 2) is faster than the rotation of the hexagonal structure (filled circles).

The dependence of the angle of rotation on distance is not linear because in the course of propagation the background beam spreads out and the distance between the vortices increases. That causes a decrease of the angular velocity with increasing propagation length.

Similar behavior was described previously for Kerr nonlinearity.<sup>33</sup> Here we point out the effects of saturation of the nonlinearity. As was already mentioned, the rotation of the lattice and the increased beam spreading in the case of equal TCs are topological effects. The effects that depend on nonlinearity are related to the local intensity by means of the specific beam shape and the intensity pattern formed on the background. For example, the transverse profile of a single OVS in a saturable medium differs significantly at different values of the saturation parameter<sup>26</sup> (the OVS is broader at higher saturation). In the case of periodically ordered vortices, when each individual dark beam starts to broaden, the overlap with the wings of its neighbors increases, whereas the individual cores do not change significantly. Because the vortices are superimposed upon a finite background beam whose total energy is conserved, bright peaks form between the vortices as a result of local energy redistribution [Fig. 1(c), bottom]. Therefore, even in a saturable medium, sharp intensity changes are present. These intensity variations reflect in a well-defined periodic modulation of the refractive index of the medium is still preserved.

### 3. EXPERIMENTAL INVESTIGATION

The experimental setup is similar to one used previously<sup>32,49</sup> and is shown in Fig. 3. We used the 488-nm line from an Ar<sup>+</sup> laser to reconstruct the photolithographically produced CGH with the desired vortex lattice. The +1 (or -1) order of the diffraction was separated from the other diffraction orders by an iris diaphragm and was focused on the input face of a glass cell containing the NLM. The output face of the cell was imaged to a CCD camera, and neutral filters were used to prevent its saturation.

To ensure the correct generation of the lattices by the CGHs, first we opened the diaphragm, allowing the +1 diffraction order to interfere with the plane 0th order. Interference patterns for three lattices are presented in Fig. 4. The vortices appear as forks of interference lines. Two neighboring vortices at each image are marked with

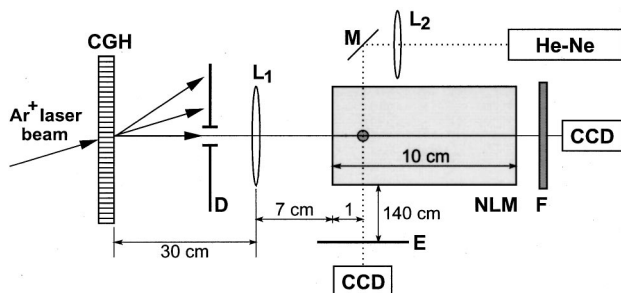


Fig. 3. Experimental setup: D, iris diaphragm; L<sub>1</sub>, L<sub>2</sub>, lenses of focal lengths 7.0 and 8.0 cm, respectively; M, mirror; E, screen; F, neutral-density filters; CCD, camera. The characteristic distances between elements are shown.

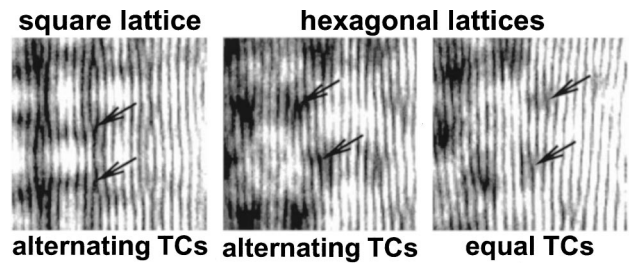


Fig. 4. Interferograms of three experimentally generated lattices. Two neighboring vortices in each image are marked with arrows.

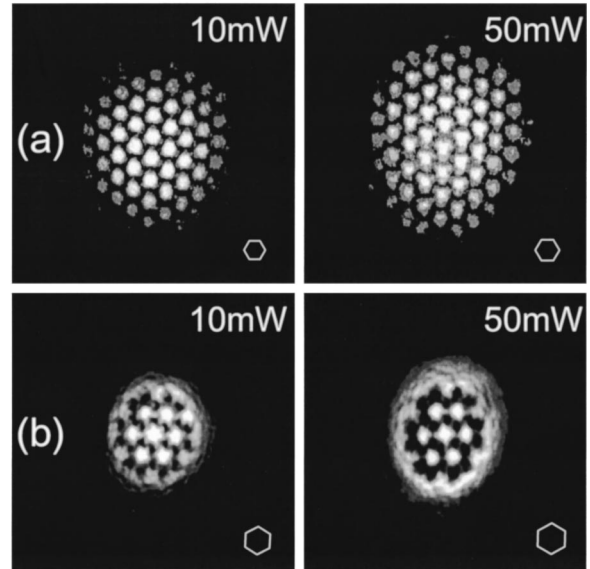


Fig. 5. Experimental images of the vortex lattices after 10-cm propagation in a NLM. (a) Hexagonal lattice with alternating TCs for powers of 10 and 50 mW. (b) Hexagonal lattice with equal TCs for the same powers. The inset in each image represents the size and the orientation of the elementary cell of each lattice.

arrows. The images show a correctly reproduced square-shaped lattice with alternating TCs and two hexagonal lattices with alternating and equal TCs (Fig. 4, left to right). The images are brighter on the right-hand side because they inhomogeneously overlapped the 0th-order beam. That inhomogeneity also introduced an intensity gradient into the structure of vortices, which caused shrinking and displacement of the vortices from their regular positions. Overall, that effect led to deformation of the lattice. Being aware of this fact, in the experiment we preserved the regular lattice structure by placing the diaphragm as close as possible to the CGH.

We determined the features of the nonlinear propagation by measuring the characteristic nonlinear parameters of the medium for two dye concentrations. For the lower concentration, the power necessary for forming a one-dimensional dark-soliton stripe was estimated to be  $P_{1Dsol} \approx 22$  mW, and the saturation power was  $P_{sat} \approx 60$  mW (measured in a self-bending scheme).<sup>49</sup> For the higher concentration the characteristic powers were  $P_{1Dsol} \approx 20$  mW and  $P_{sat} \approx 16$  mW. The intensity distributions for two hexagonal lattices (with alternating and equal charges) at the end of the NLM with the lower

dye concentration are shown in Fig. 5. Because of some technical restrictions in synthesizing the CGH, for the lattice with equal TCs the number of vortices encoded is less than in the hologram with alternating TCs. The geometrical characteristics (the elementary cell of the lattices), however, are the same in both cases. The propagation behavior for the two lattices is clearly different. Whereas the lattice with alternating charges exhibits steady propagation [Fig. 5(a)], the lattice with equal charges [Fig. 5(b)] tends to rotate (at  $\sim 28^\circ$  counterclockwise). The background beam spread more widely than in the case of a lattice with alternating charges. Unfortunately, because of the different number of vortices, this fact is not obvious from Fig. 5. The smaller number of vortices in Fig. 5(b) modulates the background beam such that more filters were used to prevent saturation of the CCD camera. As a consequence, the wings of the background beam in Fig. 5(b) are not seen, and the beam diameter seems to be smaller than in Fig. 5(a). To illustrate that the spreading is indeed greater for equal TCs we examined in detail the size of the elementary cell of the honeycomb lattice. Because the distances between the neighboring vortices were encoded in the CGHs to be the same (the holograms produced were inspected by a microscope), any difference in vortex separation is due to evolution during propagation. Of the images in Fig. 5 we inset the exact size and orientation of the elementary hexagonal cell of the lattice (see the bottom-right corner of each image). Indeed, a comparison of the elementary cells of the lattices for the two cases shows that the one with equal TCs is 18% larger.

The influence of nonlinearity can be seen if the corresponding images for two powers are compared. We note again that an increase in beam power does not influence the degree of rotation of the lattice presented in Fig. 5(b) because the waist of the laser beam is near the input face of the NLM. The higher power of the laser beam contributes, however, to broadening of the background beam. Comparing the sizes of the elementary cell of the same lattice at two different powers, we estimated 15% broadening of the beam for Fig. 5(a) and 12% for Fig. 5(b). That difference we attributed to the increased background beam size at the entrance of the NLM, which is due to the topological interaction of the equally charged vortices between the CGH and the NLM.

The square-shaped lattices were investigated in the same way, and qualitatively similar features were observed. We also investigated lattices with intentionally encoded defects in their structures, e.g., when one of the vortices is missing or all the vortices in a line are shifted out of their equilibrium position. These experiments revealed the interesting property that the lattices exhibit elasticity. However, the resolution in our experiments was not sufficient to enable us to resolve this feature in more than a qualitative manner.

#### 4. DIFFRACTION OF A PROBE BEAM BY VORTEX LATTICES

When an intense laser beam propagates along a NLM, its refractive index changes proportionally to the intensity distribution. Inasmuch as the vortex lattices possess a

periodic intensity distribution (see Figs. 1 and 5) one can expect periodic modulation of the refractive index. In a self-defocusing medium the higher local intensity will correspond to a lower local refractive index. The lattices are imposed on a finite background beam, which induces in the NLM a cylindrical defocusing lens (considered perpendicular to the laser beam). This lens is modulated by the dark-vortex structure that constitutes the lattice. In a thermal NLM, such as slightly absorbing liquid, the non-local effect that comes from the heat transfer also influences the refractive-index change and effectively decreases its modulation. Nonlocality is not taken into account in the model of Eq. (1). Its manifestation is that at zero intensity (the points of vortex phase dislocation) the refractive-index change is nonzero (see a description in Ref. 50).

To investigate the modulation of the refractive index in the NLM caused by the presence of lattices we conducted an experiment in which a (probe) single-mode He-Ne laser beam was directed perpendicularly to the (pump)  $\text{Ar}^+$  laser beam, as shown in Fig. 3. We aligned the probe beam such that it crossed the pump beam 1 cm inside the NLM. (The higher dye concentration was used in this experiment.) The input profile of the He-Ne beam is shown in Fig. 6 [image (a)], and its circular symmetry is evident. When it crossed the  $\text{Ar}^+$  laser beam the symme-

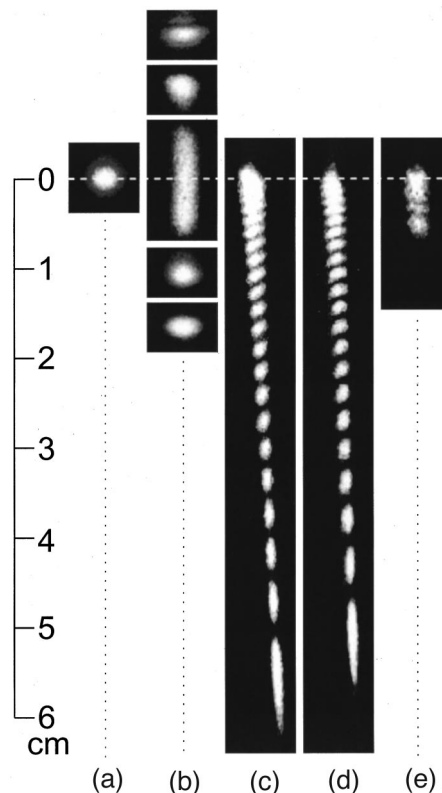


Fig. 6. Images of the probe He-Ne laser beam on screen E (Fig. 3). (a) Input He-Ne laser beam profile; (b) intensity profiles of the probe beam at low pump power (10 mW) for different vertical displacements with respect to the pump beam; (c), (d) diffraction of the He-Ne beam from periodic phase gratings induced in the NLM by square and hexagonal lattices, respectively (pump power, 80 mW); (e) diffraction pattern when a single vortex is superimposed upon the pump beam (pump power, 30 mW).

try was distorted and the beam was elongated in the direction perpendicular to the plane of Fig. 3.

First we identified the effect of an optically induced Gaussian cylindrical lens on the probe beam. To keep the same background beam characteristics, we shifted the CGH such that only a region with parallel interference lines was illuminated, thus ensuring an unmodulated background beam. This unmodulated pump beam induced a cylindrical lens in the NLM, whereas the probe beam passed through the lens and was defocused [Fig. 6, center of images (b)]. The diameters of the two beams were estimated to be approximately equal at the cross point. Therefore one should expect that the probe beam would be strongly affected by aberrations of the induced lens. In images (b) of Fig. 6, five probe beam profiles are shown, for different positions of the He–Ne laser beam. The pump power was kept at 10 mW. Different input positions of the probe beam are achieved by parallel vertical translation by a simple periscopic system denoted, for simplicity, mirror M in Fig. 3. The He–Ne laser beam is elongated symmetrically if it crosses the pump in the center and asymmetrically if it is shifted up or down. At higher powers the aberration of the induced cylindrical lens becomes vertically asymmetric, probably as a result of the asymmetric heat diffusion in the cell.

The situation is different when the vortex lattice is imposed on the background beam. At a power of the Ar<sup>+</sup> laser beam higher than 20 mW, the vortices will have well-confined cores. Because of the nonlinear change in the refractive index, the vortex lattice writes a phase grating in the NLM. The perpendicularly propagating He–Ne laser beam passes through this grating and develops well-pronounced diffraction orders at the output screen, as shown in Fig. 6, images (c) and (d), at 80-mW pump power. The constant of the phase grating written is apparently different for the square-shaped [Fig. 6, image (c)] and for the hexagonal-shaped [Fig. 6, image (d)] lattices. In the first case the period of the vortex structure was smaller (so was the period of the phase grating) and higher dispersion in the diffraction orders was observed (higher angle of diffraction). At lower powers diffraction orders were also observed. However, it was more difficult to distinguish them at the screen because the effective cylindrical lens had a larger focal length. At different powers the magnitudes of the refractive index and the modulation depths of the phase grating written in the NLM were different. These differences influenced the energy redistribution among the diffraction orders. Moreover, because of the finite number of vortices in the lattices and the nearly equal sizes of the pump and the probe beams, diffraction from the phase grating could not be compared directly with diffraction from an infinite periodic structure. In our opinion the ratio between the intensities of the different diffraction orders is gradually influenced by the fact that different parts of the probe beam pass through different numbers of vortices. Further, at the exit of the phase grating the modulated probe beam is additionally affected by aberration of the thermal lens.

To ensure that the observed diffraction structure is in fact induced by the periodicity of the vortex lattices, we tested the diffraction caused by a single vortex superimposed upon the background beam. As shown in Fig. 6

[image (e)], diffraction by a single vortex is substantially different from and resembles the diffraction of a laser beam by a wire. In all our experiments we observed strong vertical asymmetry of the probe-beam diffraction pattern, which always developed downward at powers higher than 20 mW. Numerical modeling of the processes and further experimental investigations should allow us to gain deeper insight in the relative strengths of the mechanisms described.

## 5. CONCLUSIONS

In conclusion, we have successfully experimentally generated lattice structures of optical vortices with different topological charge distributions and described their propagation in saturable nonlinear media. Because of the intensity dependence of the refractive index these lattices induce periodic modulation of the refractive index of the medium and write an effective phase grating in it. The modulation is sufficient to force the perpendicularly propagating probe beam of a He–Ne laser to diffract. This property could appear to offer the interesting possibility of creating periodic structures in the refractive index of a NLM. It could find an application for optical writing of two-dimensional photonic crystals and could appear to be relevant to the physics of Bose–Einstein condensates.

## ACKNOWLEDGMENTS

A. Dreischuh thanks the Alexander-von-Humboldt foundation for a fellowship and for facilitating the measurements that he made at the Max-Planck-Institut für Quantenoptik (Garching, Germany). The research of D. Neshev was partially supported by a Marie-Curie individual fellowship under contract HPMFCT-2000-00455. The authors thank Yu. Kivshar, L. Torner, A. Desyatnikov, and N. Herschbach for valuable discussions and support of this research.

## REFERENCES

1. See, e.g., M. Vasnetsov and K. Staliunas, eds., *Optical Vortices* (Nova Science, New York, 1999).
2. J. F. Nye and M. V. Berry, "Dislocations in wave trains," *Proc. R. Soc. London, Ser. A* **336**, 165–190 (1974).
3. A. Mair, A. Vaziri, G. Weihs, and A. Zeilinger, "Entanglement of the orbital angular momentum states of photons," *Nature* **412**, 313–316 (2001).
4. See, e.g., R. J. Donnelly, *Quantized Vortices in Helium II* (Cambridge U. Press, Cambridge, 1991).
5. J. E. Williams and M. J. Holland, "Preparing topological states of a Bose–Einstein condensate," *Nature* **401**, 568–572 (1999).
6. M. R. Matthews, B. P. Anderson, P. C. Haljan, D. S. Hall, C. E. Wieman, and E. A. Cornell, "Vortices in a Bose–Einstein condensate," *Phys. Rev. Lett.* **83**, 2498–2501 (1999).
7. P. Couillet, L. Gil, and F. Rocca, "Optical vortices," *Opt. Commun.* **73**, 403–408 (1989).
8. M. W. Beijersbergen, R. P. C. Coerwinkel, M. Kristiasen, and J. P. Woerdman, "Helical-wave-front laser-beams produced with a spiral phaseplate," *Opt. Commun.* **112**, 321–327 (1994).
9. Chr. Tamm and C. O. Weiss, "Bistability and optical switching of spatial patterns in a laser," *J. Opt. Soc. Am. B* **7**, 1034–1038 (1990).

10. D. V. Petrov, F. Canal, and L. Torner, "A simple method to generate optical beams with a screw phase dislocation," *Opt. Commun.* **143**, 265–267 (1997).
11. N. R. Heckenberg, R. McDuff, C. P. Smith, and A. G. White, "Generation of optical phase singularities by computer-generated holograms," *Opt. Lett.* **17**, 221–223 (1992).
12. I. V. Basisty, V. Y. Bazhenov, M. S. Soskin, and M. V. Vashnetsov, "Optics of light beams with screw dislocations," *Opt. Commun.* **103**, 422–428 (1993).
13. I. Freund, "Critical point explosions in two-dimensional wave fields," *Opt. Commun.* **159**, 99–117 (1999).
14. K. Staliunas, "Vortices and dark solitons in two-dimensional nonlinear Schrödinger equation," *Chaos, Solitons Fractals* **4**, 1783–1796 (1994).
15. G. Molina-Terriza, E. M. Wright, and L. Torner, "Propagation and control of noncanonical optical vortices," *Opt. Lett.* **26**, 163–165 (2001).
16. G. Molina-Terriza, J. Recolons, J. P. Torres, L. Torner, and E. M. Wright, "Observation of the dynamical inversion of the topological charge of an optical vortex," *Phys. Rev. Lett.* **87**, 023902 (2001).
17. D. Rozas, C. T. Law, and G. A. Swartzlander, Jr., "Propagation dynamics of optical vortices," *J. Opt. Soc. Am. B* **14**, 3054–3065 (1997).
18. D. Rozas, Z. S. Sacks, and G. A. Swartzlander, Jr., "Experimental observation of fluidlike motion of optical vortices," *Phys. Rev. Lett.* **79**, 3399–3402 (1997).
19. Yu. S. Kivshar, J. Christou, V. Tikhonenko, B. Luther-Davies, and L. M. Pismen, "Dynamics of optical vortex solitons," *Opt. Commun.* **152**, 198–206 (1998).
20. J. Christou, V. Tikhonenko, Y. S. Kivshar, and B. Luther-Davies, "Vortex soliton motion and steering," *Opt. Lett.* **21**, 1649–1651 (1996).
21. Yu. S. Kivshar and B. Luther-Davies, "Dark optical solitons: physics and applications," *Phys. Rep.*, **298**, 172–185 (1998).
22. A. W. Snyder, L. Poladian, and D. J. Mitchell, "Stable dark self-guided beams of circular symmetry in a bulk Kerr medium," *Opt. Lett.* **17**, 789–791 (1992).
23. A. H. Carlsson, J. N. Malmberg, D. Anderson, M. Lisak, E. A. Ostrovskaya, T. Alexander, and Yu. S. Kivshar, "Linear and nonlinear waveguides induced by optical vortex solitons," *Opt. Lett.* **25**, 660–662 (2000).
24. C. T. Law, X. Zhang, and G. A. Swartzlander, Jr., "Waveguiding properties of optical vortex solitons," *Opt. Lett.* **25**, 55–57 (2000).
25. G. A. Swartzlander, Jr., and C. T. Law, "Optical vortex solitons observed in Kerr nonlinear media," *Phys. Rev. Lett.* **69**, 2503–2506 (1992).
26. V. Tikhonenko, Yu. S. Kivshar, V. V. Steblina, and A. A. Zozulya, "Vortex solitons in a saturable optical medium," *J. Opt. Soc. Am. B* **15**, 79–86 (1998).
27. G. Duree, M. Morin, G. Salamo, M. Segev, B. Crosignani, P. Di Porto, E. Sharp, and A. Yariv, "Dark photorefractive spatial solitons and photorefractive vortex solitons," *Phys. Rev. Lett.* **74**, 1978–1981 (1995).
28. Z. Chen and M. Segev, "Self-trapping of an optical vortex by use of the bulk photovoltaic effect," *Phys. Rev. Lett.* **78**, 2948–2951 (1997).
29. P. Di Trapani, W. Chinaglia, S. Minardi, A. Piskarskas, and G. Valiulis, "Observation of quadratic optical vortex solitons," *Phys. Rev. Lett.* **84**, 3843–3846 (2000).
30. A. V. Mamaev, M. Saffman, and A. A. Zozulya, "Decay of high order optical vortices in anisotropic nonlinear optical media," *Phys. Rev. Lett.* **78**, 2108–2111 (1997).
31. I. Velchev, A. Dreischuh, D. Neshev, and S. Dinev, "Multiple-charged optical vortex solitons in bulk Kerr media," *Opt. Commun.* **140**, 77–82 (1997).
32. A. Dreischuh, G. G. Paulus, F. Zacher, F. Grabson, D. Neshev, and H. Walther, "Modulational instability of multiple-charged optical vortex solitons under saturation of the nonlinearity," *Phys. Rev. E* **60**, 7518–7524 (1999).
33. D. Neshev, A. Dreischuh, M. Assa, and S. Dinev, "Motion control of ensembles of ordered optical vortices generated on finite extent background," *Opt. Commun.* **151**, 413–421 (1998).
34. B. Luther-Davies, R. Powles, and V. Tikhonenko, "Nonlinear rotation of three-dimensional dark spatial solitons in a Gaussian laser beam," *Opt. Lett.* **19**, 1816–1818 (1994).
35. D. Rozas and G. A. Swartzlander, Jr., "Observed rotational enhancement of nonlinear optical vortices," *Opt. Lett.* **25**, 126–128 (2000).
36. G.-H. Kim, J.-H. Jeon, Y.-Ch. Noh, K.-H. Ko, H.-J. Moon, J.-H. Lee, and J.-S. Chang, "An array of phase singularities in a self-defocusing medium," *Opt. Commun.* **147**, 131–137 (1998).
37. G. M. McDonald, K. S. Syed, and W. J. Firth, "Dark spatial soliton break-up in the transverse plane," *Opt. Commun.* **95**, 281–288 (1993).
38. V. Tikhonenko, J. Christou, B. Luther-Davies, and Yu. S. Kivshar, "Observation of vortex solitons created by the instability of dark soliton stripes," *Opt. Lett.* **21**, 1129–1131 (1996).
39. A. V. Mamaev, M. Saffman, and A. A. Zozulya, "Propagation of dark stripe beams in nonlinear media: snake instability and creation of optical vortices," *Phys. Rev. Lett.* **76**, 2262–2265 (1996).
40. D. Neshev, A. Nepomnyashchy, and Yu. S. Kivshar, "Nonlinear Aharonov–Bohm scattering for optical vortices," *Phys. Rev. Lett.* **87**, 043901 (2001).
41. G. Molina-Terriza and L. Torner, "Reconfigurable dynamic beam shaping in seeded frequency doubling," *Opt. Lett.* **26**, 154–156 (2001).
42. G. S. McDonald, K. S. Syed, and W. J. Firth, "Optical vortices in beam propagation through a self-defocusing medium," *Opt. Commun.* **94**, 469–476 (1992).
43. S. W. Leonard, J. P. Mondia, H. M. van Driel, O. Toader, S. John, K. Busch, A. Birner, U. Gösele, and V. Lehmann, "Tunable two-dimensional photonic crystals using liquid-crystal infiltration," *Phys. Rev. B* **61**, R2389–R2392 (2000).
44. K. T. Gahagan and G. A. Swartzlander, Jr., "Optical vortex trapping of particles," *Opt. Lett.* **21**, 827–829 (1996).
45. Ch. Slinger, P. Brett, V. Hui, G. Monnington, D. Pain, and I. Sage, "Electrically controllable multiple, active, computer-generated hologram," *Opt. Lett.* **22**, 1113–1115 (1997).
46. K. W. Madison, F. Chevy, W. Wohlleben, and J. Dalibard, "Vortex formation in a stirred Bose–Einstein condensate," *Phys. Rev. Lett.* **84**, 806–809 (2000).
47. B. P. Anderson, P. C. Haljan, C. A. Regal, D. L. Feder, L. A. Collins, C. W. Clark, and E. A. Cornell, "Watching dark solitons decay into vortex rings in a Bose–Einstein condensate," *Phys. Rev. Lett.* **86**, 2926–2929 (2001).
48. J. R. Abo-Shaeer, C. Raman, J. M. Vogels, and W. Ketterle, "Observation of vortex lattices in Bose–Einstein condensates," *Science* **292**, 476–479 (2001).
49. A. Dreischuh, D. Neshev, G. G. Paulus, and H. Walther, "Experimental generation of steering odd dark beams of finite length," *J. Opt. Soc. Am. B* **17**, 2011–2017 (2000).
50. A. M. Deykoon and G. A. Swartzlander, Jr., "Pinched optical-vortex soliton," *J. Opt. Soc. Am. B* **18**, 804–810 (2001).